

DEVELOPMENT OF A SPRING MODEL FOR THE STRUCTURAL ANALYSIS OF A DOUBLE-LAYERED TIMBER PLATE STRUCTURE WITH THROUGH-TENON JOINTS

Anh Chi Nguyen¹, Yves Weinand²

ABSTRACT: Timber plate structures with integral mechanical attachments have been successfully built in the last decades. Previous research has highlighted the influence of these connections in the global behavior of the structures. Double-layered plate shells are one of the latest applications of integral joints. Their fabrication and assembly has been proven efficient. However, their structural behavior remains unknown. Simplified models are required to predict their behavior since an individual detailed modelling of the large amount of joints would be time-consuming and computationally expensive. Current simplifications involve either considering the connections as rigid or hinged and do not allow accurate prediction of their behavior. In this paper, a numerical finite element model in which the semi-rigid behavior of the joints is modeled by means of springs is presented for a double-layered timber plate structure made of 5 by 3 segments. The numerical model is automatically generated in the finite element software Abaqus™ from a simplified geometry. Numerical results are compared to a three-point bending test performed on two specimens. The developed spring model shows promising results for its application to a full double-layered timber plate shell. Only axial and shear stiffnesses were implemented in this model while the other degrees of freedom were considered rigid. This consideration might lead to an overly stiff model.

KEY WORDS: timber plate structure, through-tenon joint, mechanical behavior, finite element spring model

1 INTRODUCTION

With the development of new fabrication technology and rising demand for environmentally sound structures, computer-numerical-control (CNC)-fabricated integral mechanical attachments have shown an increasing interest among researchers. Inspired by traditional woodworking joints like dovetail and finger joints, they have recently been used in several applications such as segmental plate shells (e.g. *ICD/ITKE Research Pavilion 2010* [1] and *Landesgartenschau Exhibition Hall* [2]) and folded plate structures (e.g. *Lausanne Vidy theatre* [3]). These structures are composed by a large amount of discrete thin timber panels mutually connected by integral joints along their edges. Successively improved from single tab-and-slot joint to multiple tab-and-slot joints and from 1-plane joints to 2-plane joints, single-degree-of-freedom (1-DOF) multiple tab-and-slot joints (MTSJ) have finally been developed [4].

Local and global studies have been carried out on MTSJ. The former have analyzed the influence of different joint's geometries on their shear and bending resistance

and have shown the advantage of closed-slot joints, also referred as through-tenon joints, providing better rotational stiffness with same high shear capacity, in comparison with open-slot joints [5]. Applied to folded plate structures, their influence on the global structural behavior has been subsequently investigated and the semi-rigid behavior of MTSJ has been highlighted. Moreover, tests have shown that lightweight structures with high load-bearing capacity could be built with MTSJ without requiring mechanical fasteners and glue [6].

One of the latest applications of integral joints in timber shell structures are double-layered timber plate shells presented in Robeller *et al.* [7]. These structures use multiple tab-and-slot through-tenon joints (MTSJ-TT). If their construction has been proven successful, their global behavior, substantially influenced by their semi-rigid connections, remains difficult to predict.

The main objective of this paper is to present the development of a pertinent numerical model allowing the prediction of the global behavior of double-layered timber plate shells. The finite element method (FEM) was used and the semi-rigid behavior of MTSJ was considered by modeling them as springs, such as applied for segmental plate shells [2] and folded plate structures [6]. Three-point bending tests were performed to identify the failure modes of the structure and assess the numerical model. These experimental tests were carried

¹ Anh Chi Nguyen, Laboratory for Timber Constructions (IBOIS), Swiss Federal Institute of Technology (EPFL), anhchi.nguyen@epfl.ch

² Yves Weinand, Laboratory for Timber Constructions (IBOIS), Swiss Federal Institute of Technology (EPFL), yves.weinand@epfl.ch

out at the Laboratory for Timber Constructions (IBOIS), Swiss Federal Institute of Technology Lausanne (EPFL), on part of a double-layered timber plate shell with a simplified geometry.

2 STRUCTURAL DESIGN

2.1 CONSTRUCTION SYSTEM

The construction system of the studied structure, developed in Robeller *et al.* [7], is presented in Figure 1. The double-curved shell is formed by juxtaposed segments, each segment being made of four plates. The horizontal plates L_1 and L_2 form the two layers of the structure and the vertical plates W_0 and W_1 are added to connect the layers of one segment to the neighboring segments. These vertical plates are required due to the large dihedral angle between the horizontal plates forming each of the two layers. They are connected along their shared edge by dovetail joints. Panels are then assembled according to the vector of insertion defined by their 1DOF connections and blocked by the interlocking with the other panels. This interlocking is assumed to improve both load-bearing capacity and resistance of the global structure.

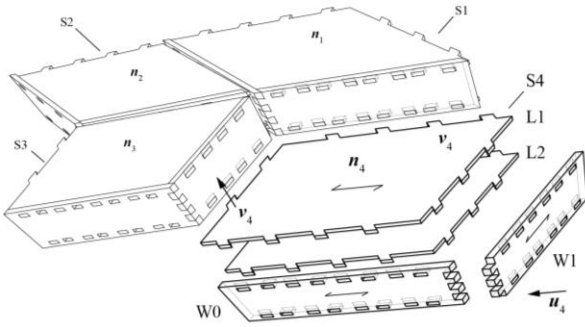


Figure 1: Construction system of the double-layered timber plate shell [7]



Figure 2: Double-layered timber plate vault prototype of the Multipurpose Hall Project (Annen SA, Manternach), scale 1:2 (12.5m span)

The case study associated with this research is the Multipurpose Hall Project of Annen SA. It consists of a roof structure made of 23 double-curved vaults with spans ranging from 22 to 53 m. A first prototype (scale 1:2) has been successfully constructed to verify its feasibility (Figure 2).

2.2 THROUGH-TENON JOINTS

In this structure, most connections are MTSJ-TT. They connect plates of the two layers together through vertical panels. These close-slot joints are 1-DOF joints whose geometry is defined by three Bryant angles θ_1 , θ_2 and θ_3 [4].

2.3 MATERIAL

In comparison with the previous prototype presented in [7], 40-mm thick BauBuche Q panels were used for the tested specimens. These panels are beech laminated veneer lumber (LVL) panels made of 14 layers of 3mm thick peeled-veneer, among which 2 layers are glued crosswise with the layup III-III-III-III (I for longitudinal, -- for crosswise veneer layer). Material properties used for the numerical model are presented in Table 1. Modulus and density values were taken from the declaration of performance of these panels provided by Pollmeier Massivholz GmbH & Co [8]. Missing values were retrieved from Pot *et al.* [9] and Sandhaas [10]. The fiber orientation of the panels is shown in Figure 1.

Table 1: Material properties of 40mm-thick BauBuche Q panels

Property	Value	Unit
Elastic modulus E_{11}	13200	N/mm ²
Elastic modulus E_{22}	2200	N/mm ²
Elastic modulus E_{33}	2200	N/mm ²
Shear modulus G_{12}	820	N/mm ²
Shear modulus G_{13}	430	N/mm ²
Shear modulus G_{23}	59	N/mm ²
Poisson's ratio ν_{12}	0.365	-
Poisson's ratio ν_{13}	0.464	-
Poisson's ratio ν_{23}	0.726	-
Density ρ_{mean}	800	kg/m ³

2.4 SIMPLIFIED GEOMETRY

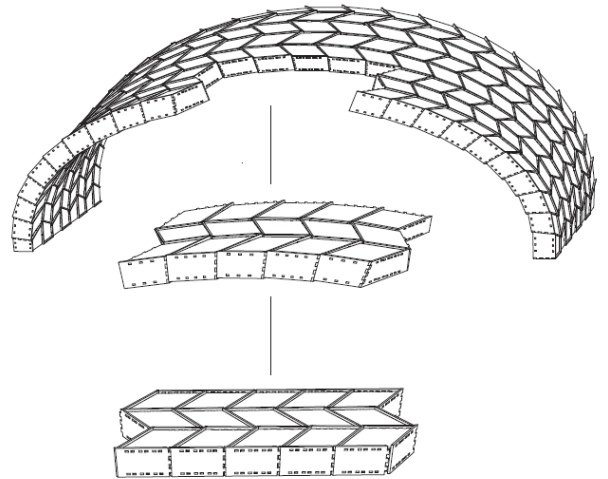


Figure 3: Simplified geometry of the tested specimens extracted from a 25-meter span vault, scale 1:1

The geometry of the tested specimens was defined according to a scale 1:1 prototype of 25-meter span. The number of segments was chosen such that at least one box was surrounded by other boxes and to reduce the side effects implied by the boundary conditions. As seen in Figure 3, 5x3 segments located at midspan were extracted from the full prototype and their geometry was simplified to eliminate the curvature. Further simplification was introduced by setting similar dimensions of the boxes per row of the prototype. The size of each segment was set to a length of 1.2m, a width of 0.85m, a static height of 0.6m and an offset equal to 80mm between the boxes. Each replicate was made of 68 plates, forming a 6.9-meter long and 2.6-meter wide prototype in total. All MTSJ-TT were set to a unique geometry, with Bryant angles $\theta_1=0^\circ$, $\theta_2=25^\circ$, $\theta_3=0^\circ$ and a tab length of 72.5mm. Additional panels were added such that the prototype was closed at all its edges.

2.5 DIGITAL FABRICATION AND ASSEMBLY

Although the fabrication of the panels has been automated [7], the assembly of the construction system is still carried out manually. Several steps are followed to obtain the final form of the structure. All segments are individually assembled and connected to each other. For each segment, the vertical panels (W_0 and W_1 in Figure 1) are first assembled and the corresponding horizontal panels (L_1 and L_2) are inserted. The individual segments are then connected one by one to form the structure vertically.

During the assembly of the tested prototypes, screws had to be added to maintain the panels in position. In fact, without the presence of screws, gaps were appearing between the panels, within each segment.

Since the prototypes were assembled vertically, lying on one of their long edges, they had to be rotated by 90° and placed on the two supports. Two threaded rods were inserted at the two ends of the 5x3 prototypes along their width to maintain the structures in position during their rotation (see Figure 4).

3 EXPERIMENTAL STUDY

3.1 TEST SETUP

Since a more sophisticated pulley-based loading system such as presented in Wong *et al.* [11] and used in Stitic *et al.* [6] would have been too cumbersome and expensive for such structure, a simpler bending test has been performed. The three-point bending test setup is illustrated in Figure 4. Load was applied at midspan using a hydraulic jack and was distributed through a beam on the three top panels located at midspan. Regarding boundary conditions, rotation was allowed along the two supported edges and horizontal translation was allowed along one edge. The supports consisted in four concrete blocks on which the steel rotulas were fixed. Two steel profiles were attached to the steel supports and were themselves screwed to the structure through timber blocks.

3.2 INSTRUMENTATION

A force transducer was placed to measure the force applied on top of the structure by the hydraulic jack. A pair of linear variable differential transformers (LVDT) were added at midspan, at both sides of the structure under the vertical panels, to measure its vertical displacement.

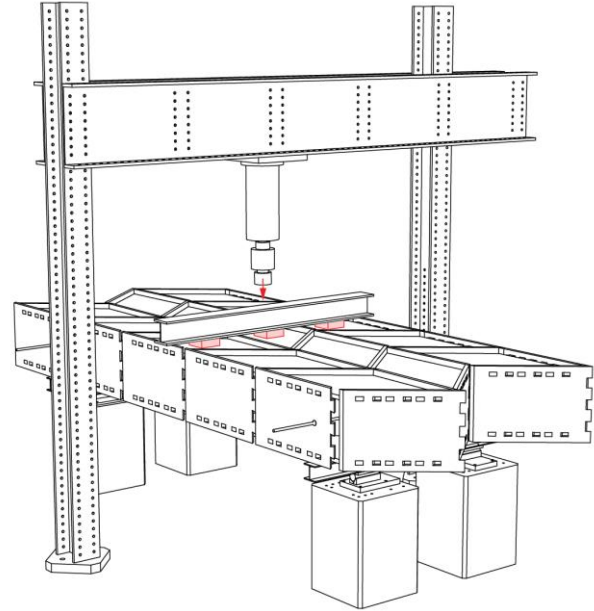


Figure 4: Three-point bending test setup

4 NUMERICAL MODEL

Due to the complexity of the structure's geometry and the large amount of connections, a pertinent model is required to predict the global behavior of the structure. Since the mathematical model cannot be solved analytically because of the form complexity, material properties of timber, boundary conditions, etc., a numerical model was developed using the finite element method. The latter is generally used to analyze plate shell structures due to its ease of implementation [6]. The geometry of the structure was simplified since a model with the exact geometry, using 3D elements for the mesh, would have been too tedious and time-consuming.

4.1 PANELS

The structure can be decomposed in discrete planar continuous elements. Therefore, plate theory was chosen to define the mathematical model. Panels were modelled as shell elements due to the small thickness-length ratio ($t/L < 0.05$) [12]. Conventional shell elements were chosen over continuum shell elements because of their ease of implementation and because through-thickness strains can be neglected since the thickness of the panels is significantly smaller to their length and width.

The material was modelled as orthotropic and linear elastic, considering a single layer of material with defined local orientations. Geometric, material and contact nonlinearities were neglected.

Finite strain S4R elements were used for the mesh. Those 4-noded 6-DOF quadrilateral elements with reduced integration were chosen for their robustness, wide application and hourglass control [13]. The mesh was refined at the vicinity of the connections where concentrations appear (seed size = 7.5mm), while a coarser mesh was used for the inner part of the panels (seed size = 50mm).

4.2 CONNECTIONS

Previous research has highlighted the importance of taking the semi-rigidity of MTSJ into account since they largely influence the behavior of the structure [6]. In the model developed, the semi-rigid behavior of MTSJ-TT was modelled by springs. A small gap (~4mm) was introduced between all plates to define the direction in which each spring is acting. Each tab was modelled by a set of $2n$ springs with 6 DOF (3 translations and 3 rotations) distributed along the length of the tab. Due to the presence of the vertical panels, springs representing through tenon joints had to be doubled to have springs at both sides of the vertical panels (see Figure 5).

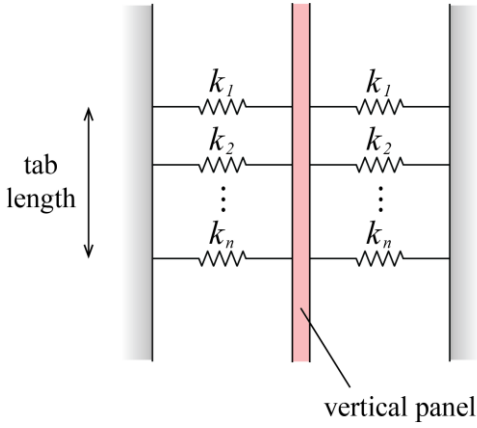


Figure 5: Schematic representation of spring connectors per tab

Each through-tenon connection with a stiffness k_{eq} was thus represented by a system of $2n$ springs in parallel and in series. The tab stiffness can be expressed in function of the individual springs k_i as shown in Equation (1). All springs having the same stiffness (Equation (2)), the stiffness of one tab can be simplified (Equation (3)) and the stiffness of each spring can then be deduced (Equation (4)).

$$k_{eq} = \frac{1}{\frac{1}{\sum_{i=1}^n k_i} + \frac{1}{\sum_{i=1}^n k_i}} = \frac{\sum_{i=1}^n k_i}{2} \quad (1)$$

$$k_i = k, \quad i = 1, \dots, n \quad (2)$$

$$k_{eq} = \frac{n \cdot k}{2} \quad (3)$$

$$k = \frac{2 \cdot k_{eq}}{n} \quad (4)$$

The axial and shear semi-rigidities of the through-tenon connections were implemented using the values presented in Table 1. Those values were retrieved from small-scale tests without considering the contribution of the screws added for the assembly of the structure [14][15]. The remaining DOF were set to a high stiffness value to be considered as rigid ($k_{rigid}=10^{12}$ N/mm). Springs were considered as being uncoupled.

Table 2: Springs stiffnesses values per tab of the MTSJ-TT connection used in the numerical model

Property	Value	Unit
Axial stiffness	11604.0	N/mm
Shear stiffness 12	19009.4	N/mm

In the upper graph in Figure 6, the number of spring connectors n influences the vertical displacements. The use of one spring per connector on each side of the vertical panel leads to an overly flexible structure and thus overestimated displacements. Increasing the number of connectors converges to more accurate results. However, the computation time drastically increases for a high number of connectors. For the reduced prototype of 5x3 segments, 2x7 springs per connectors were used. However, a maximum number of 2x3 springs will be used for the modeling of the arches.

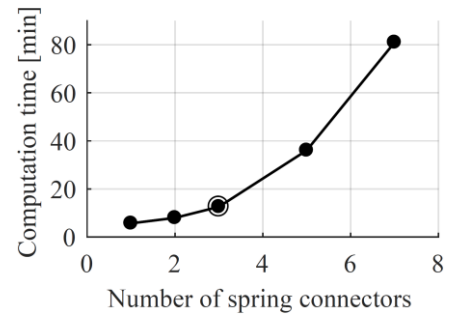
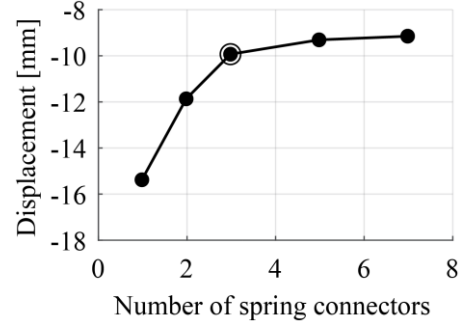


Figure 6: Vertical displacement and computation time vs. number of spring connectors on each side of the vertical panel

Dovetail connections along the vertical plates were considered as being rigid and were modelled as tied connections since their rotation is blocked by the interlocking of the panels.

4.3 BOUNDARY CONDITIONS

Boundary conditions were modelled by single rectangle plates with properties equivalent to the actual supports of

the setup. These plates were modeled as rigid bodies with the center of rotation of the supports assigned as reference nodes. The nodes at the contour of these plates were set as tie-type nodes assigned to the rigid body such that their translational and rotational DOF were associated with the rigid body. Coupling kinematic constraints were then set between the reference nodes and the nodes located on the structure that are resting on the supports for all DOF. The pinned and roller constraints were then assigned to the reference nodes.

4.4 FEM GEOMETRY

To generate the numerical model and implement all the spring connections in the FE software, the midsurfaces representing the panels are partitioned to have mesh nodes at the exact positions where the panels are connected by springs. Each panel, horizontal or vertical, is represented by a polysurface and the entire FEM geometry of the structure can be represented by a set of polysurfaces.

4.5 AUTOMATIC GENERATION

Due to the large amount of connections in the structure, a code has been developed to generate automatically the numerical FE model. The manual implementation of the definition all spring connections more specifically would have been too tedious. In fact, the prototype of 5x3 segments already contains 360 through-tenon connections, equivalent to 624 sets of springs because of the doubling of the connections due to the vertical panels. For sets of 3 springs with 6 DOF, 11 232 values need to be assigned to the connections.

The automatic generation of the numerical model was achieved using the Abaqus Scripting Interface. The FEM geometry was directly imported from the computer aided design (CAD) software in an ACIS format (.sat). The Python scripts written in this interface include the importation of the geometry, materials and sections definitions, assembly of all parts, mesh generation, steps generation, interactions definitions (i.e. definition of all springs with their local coordinate systems), loads application as well as boundary conditions. Automatic generation has the advantage to allow fast change of the values of springs stiffnesses, mesh elements size, loads, boundary conditions, etc.

5 RESULTS AND DISCUSSION

5.1 EXPERIMENTAL TESTING

Vertical displacements measured by LVDT sensors at midspan for the tested specimens are presented in Figure 6. Failure was reached for surcharge loads of 115.4kN and 100.8kN and occurred for both specimens at the through-tenon joints connecting neighboring segments at the bottom layer. As we can see, there is a large dispersion of results obtained for the two tested specimens.

It can be noted that the load measured by the LVDT sensors and indicated in Figure 7 is the load applied on top of the structure, additionally to gravity and the weight of the distributing beam.

The failure of the joints was due to a combination of shear and traction, as shown in Figure 8. Dovetail joints connecting the vertical panels appeared to be undamaged, supposing that the hypothesis of rigid dovetail joints in the numerical model can be assumed to model the behavior of the structure since the rotation of these connections is blocked by the interlocking of the panels.

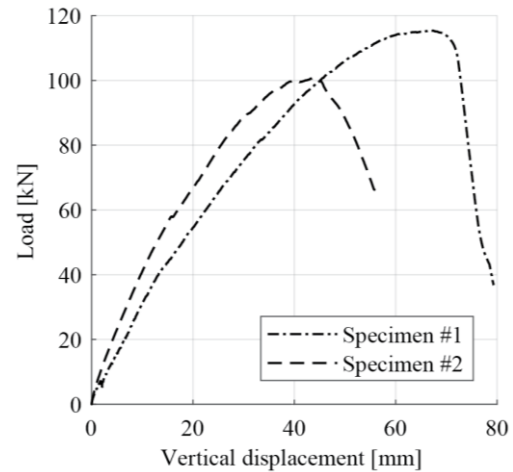


Figure 7: Load vs. midspan deflection of the two specimens

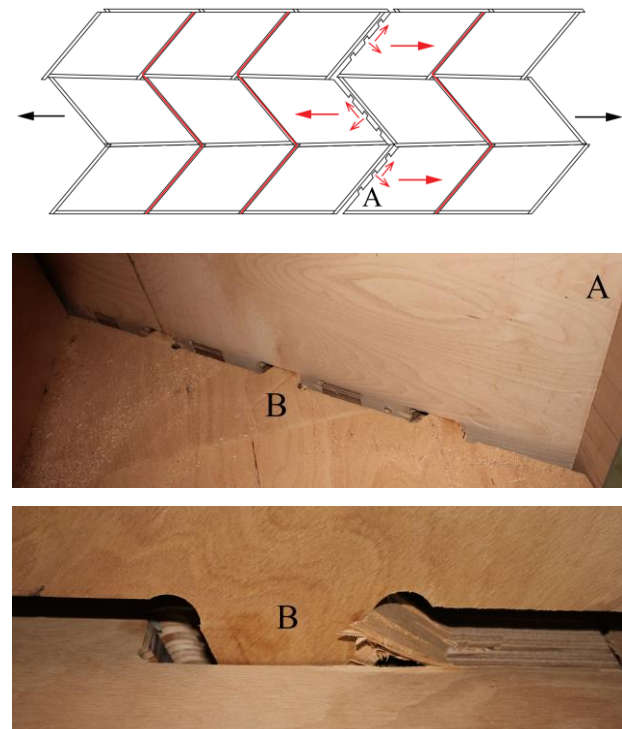


Figure 8: Failure of the MTSJ-TT at the bottom layer of the structure connecting segments together due to a combination of shear and traction

5.2 NUMERICAL MODEL

Figure 9 presents the obtained model in the FE software Abaqus™ with all spring connections (in this case for 2x7 spring connectors per tab) and mesh properties.

Since the measurements were taken after the structure was placed on the supports, initial displacements due to gravity were not recorded. Therefore, to compare both experimental and numerical results, the first loading step where gravity only is acting was subtracted from the subsequent loading steps still considering the propagated effects of gravity.

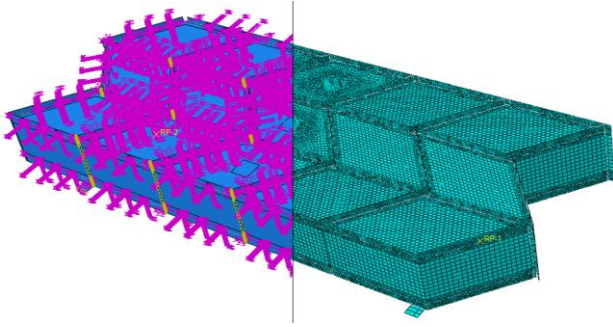


Figure 9: Numerical spring model with 2x7 springs per tab (left) and refined mesh (right)

Results of the numerical model compared to the elastic part of the experimental tests are presented in Figure 10 for an additional load of 50kN, approximately corresponding to SLS maximal displacements. The spring model is stiffer than the linear regression of the two tested specimens. However, it must be noted that since only the axial and shear stiffnesses have been implemented in the model, the current numerical model could be overly stiff.

Results were compared to a model with rigid connections by setting high stiffness values to all spring ($k_{rigid}=10^{12}$ N/mm). The stiffness obtained was $k=6.82$, which overestimates the linear regression of the experimental results by 94%.

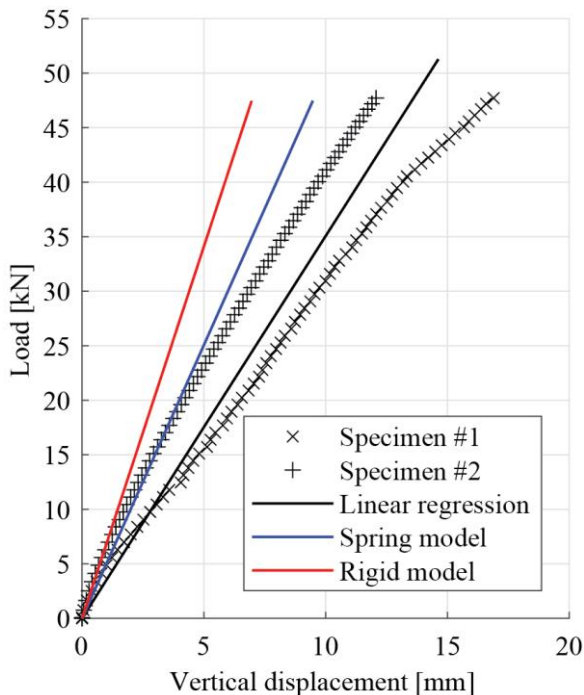


Figure 10: Load vs. displacement of the two specimens

6 CONCLUSIONS

It has been shown that joints constitute weak points of the structure, failing due to a combination of shear and traction. The semi-rigidity of the joints thus needs to be considered to predict the global behavior of the structure. The spring model seems to be relevant to model structures with complex geometries such as double-layered timber plate shells. The advantage of this method is that it can be derived from the actual 3D geometry straightforwardly.

Promising results were obtained by using this model to assess the semi-rigid behavior of double-layered timber plate structures when compared to a model with rigid connections. Results with axial and shear stiffnesses only seem to be too stiff. The implementation of the semi-rigidity for the other DOF could lead to a higher accuracy of the model.

Finally, the number of spring connectors per tab used in the model influences the quality of the model. A compromise is necessary between computational time and accuracy of the results. If a model with 2x7 springs per tab could be achieved for a small prototype of 5x3 segments, a maximum of 2x3 springs per tab would be conceivable for a full arch made of hundreds of segments.

7 OUTLOOK AND FUTURE WORK

The numerical spring model provided promising results, opening paths for further research and investigations:

- At least one additional test should be performed to confirm the pertinence of the numerical model because of the large dispersion of results obtained for the two tested specimens. However, the high costs of the specimens limit the number of samples.
- In the numerical model, only shear and axial stiffnesses were implemented. The influence of the implementation of the semi-rigidity for the other DOF has to be investigated.
- In this paper, study has been limited to the analysis of displacements. Strains analysis should be performed and compared to experimental tests by means of digital image correlation or strain gauges.
- The study has been limited to the linear elastic part. Since this model does not capture deviations from the linear approximation, geometric nonlinearity could be considered in the model. The plastic behavior of the connections has to be introduced in the spring definitions as well as the panels to predict the failure of the structure.
- The FEM geometry of the spring model can be derived straightforwardly from the 3D geometry. However, for the 5x3 segments prototype, it has been drawn manually from the 3D geometry. An automatic generation of the FEM geometry needs to be implemented for the study of full vaults since their manual drawing would be too time-consuming.
- The test setup could be revised to have a distributed load applied onto the structure.

The major outcome of further research would be the structural optimization of double-layered timber plate shells.

ACKNOWLEDGEMENT

This research was supported by the NCCR Digital Fabrication, funded by the Swiss National Science Foundation (NCCR Digital Fabrication Agreement \#51NF40-141853). The research is carried out in parallel to the Multipurpose Hall project (client: Annen SA, architect: Valentiny-Weinand) with the objective of comparing the semi-rigid spring model to the calculations performed by the Bureau d'Etudes Weinand in charge of the structural engineering.

REFERENCES

- [1] Kaltenbach F.: Teaching by Doing - A Research Pavilion in Stuttgart. *Detail (English Edition)*, 2010(6):559-561, 2010.
- [2] Li J.-M., Knippers J.: Segmental Timber Plate Shell for the Landesgartenschau Exhibition Hall in Schwäbisch Gmünd - the Application of Finger Joints in Plate Structures. *International Journal of Space Structures*, 30(2):123-140, 2015.
- [3] Robeller C., Gambero, J., Weinand, Y.: Theatre Vidy Lausanne A Double-Layered Timber Folded Plate Structure. *Journal of the International Association for Shell and Spatial Structures*, 58(4): 295-314, 2017.
- [4] Robeller C.: Integral Mechanical Attachment for Timber Folded Plate Structures. PhD thesis, École Polytechnique Fédérale de Lausanne, 2015.
- [5] Roche S., Gambero J., Weinand Y.: Multiple Tab-and-Slot Joint: Improvement of the Rotational Stiffness for the Connection of Thin Structural Wood Panels. In: *World Conference on Timber Engineering*, 1556-1564, 2016.
- [6] Stitic A., Nguyen A. C., Weinand Y.: Numerical Modelling of Semi-Rigidity of Timber Folded Surface Structures with Multiple Tab and Slot Joints. Manuscript submitted for publication.
- [7] Robeller C., Konakovic M., Dedijer M., Pauly M., Weinand Y.: A Double-Layered Timber Plate Shell - Computational Methods for Assembly, Prefabrication and Structural Design. In: *Advances in Architectural Geometry*, 104-122, 2016.
- [8] Pollmeier (2015) Declaration of Performance: Laminated veneer lumber made of beech. PM-003-2015. Available at https://www.pollmeier.com/en/dam/jcr:e2bad0e8-b111-4890-9f21-819f7ed9ebf0/Leistungserkl%C3%A4rung%20BauBuche%20Platte_PM003-2015_englisch.pdf [Verified 23 April 2018].
- [9] Pot G., Denaud L.E., Collet R.: Numerical Study of the Influence of Veneer Lathe Checks on the Elastic Mechanical Properties of Laminated Veneer Lumber (LVL) Made of Beech. *Holzforschung*, 69(3), 337-345, 2015.
- [10] Sandhaas C.: Mechanical Behaviour of Timber Joints With Slotted-In Steel Plates. PhD thesis, University of Technology Delft, 2012.
- [11] Wong H.T., Teng J. G., Wang Z. C.: A Pully-Based System for the Simulation of Distributed Loading on Shell Roof Structures. *Experimental Techniques*, 27(5):21-27, 2006.
- [12] Oñate E.: Structural Analysis with the Finite Element Method. Linear Statics, volume 2. Springer, 2013.
- [13] Dassault Systèmes (2012). Abaqus 6.12 Online Documentation. Available at <http://abaqus.software.polimi.it/v6.12/books/hhp/default.htm> [Verified 23 April 2018].
- [14] Rad A. R., Weinand Y.: [In plane-shear stiffness of through-tenon joints]. Unpublished raw data.
- [15] Nguyen A. C., Weinand Y.: [Traction stiffness of through-tenon joints]. Unpublished raw data.